

Prepared in cooperation with the U.S. Geological Survey Water Availability and Use Science Program

# MODFLOW 6 Groundwater Transport Model Example Problems

Version mf6.0.x—Xxx xx, 20171

U.S. Department of the Interior  
U.S. Geological Survey

DRAFT: December 18, 2019

—PROVISIONAL—  
This should not be referenced, cited, or  
released without USGS Bureau approval.

**Cover.** Binary computer code illustration.

DRAFT: December 18, 2019

---PROVISIONAL---

This should not be referenced, cited, or  
released without USGS Bureau approval.

# Contents

Introduction .....	1
Example Problems .....	1
Problem 1–One-Dimensional Transport .....	1
Problem 11–Henry Problem .....	7
Problem 12–Fluctuating Saltwater Boundary .....	11
Problem 13–Saltwater Intrusion Dynamics .....	15
References Cited .....	R-1

# Figures

1. Analytical (Wexler, 1992) and numerical solution (MODFLOW 6) for solute transport in a one-dimensional, steady flow field for the low dispersion case ( $\alpha_L = 0.1 \text{ cm}$ , $D_{xx} = 0.01 \text{ cm}^2/\text{s}$ ). Results are shown for three different distances (0.05, 4.05, and 11.05 cm from the end of the first cell). Every fifth time step is shown for the MODFLOW 6 results .....	2
2. Analytical (Wexler, 1992) and numerical solution (MODFLOW 6) for solute transport in a one-dimensional, steady flow field for the high dispersion case ( $\alpha_L = 1.0 \text{ cm}$ , $D_{xx} = 0.1 \text{ cm}^2/\text{s}$ ). Results are shown for three different distances (0.05, 4.05, and 11.05 cm from the end of the first cell). Every fifth time step is shown for the MODFLOW 6 results .....	2
3. Detailed view of the analytical solution and MODFLOW 6 results for early times ( $t < 10 \text{ s}$ ) at the first cell. Results are for the high dispersion case, as shown in figure 2. Every time step is shown for the MODFLOW 6 results .....	3
4. Analytical (Wexler, 1992) and numerical solution (MODFLOW 6) for solute transport in a one-dimensional, steady flow field for the low dispersion case ( $\alpha_L = 0.1 \text{ cm}$ , $D_{xx} = 0.01 \text{ cm}^2/\text{s}$ ). Results are shown for three different times (6, 60, and 120 s from the start of the simulation). Every other cell is shown for the MODFLOW 6 results .....	3
5. Analytical (Wexler, 1992) and numerical solution (MODFLOW 6) for solute transport in a one-dimensional, steady flow field for the high dispersion case ( $\alpha_L = 1.0 \text{ cm}$ , $D_{xx} = 0.1 \text{ cm}^2/\text{s}$ ). Results are shown for three different times (6, 60, and 120 s from the start of the simulation). Every other cell is shown for the MODFLOW 6 results .....	4
6. Analytical (Wexler, 1992) and numerical solution (MODFLOW 6) for solute transport in a one-dimensional, steady flow field for the low dispersion case ( $\alpha_L = 0.1 \text{ cm}$ , $D_{xx} = 0.01 \text{ cm}^2/\text{s}$ ) and with a first-order decay rate of $\lambda = 0.01 \text{ s}^{-1}$ . Results are shown for four different times (30, 60, 90, and 120 s from the start of the simulation). Every third cell is shown for the MODFLOW 6 results .....	5

7. Analytical (Wexler, 1992) and numerical solution (MODFLOW 6) for solute transport in a one-dimensional, steady flow field for the high dispersion case ( $\alpha_L = 1.0 \text{ cm}$ , $D_{xx} = 0.1 \text{ cm}^2/\text{s}$ ) and with a first-order decay rate of $\lambda = 0.01 \text{ s}^{-1}$ . Results are shown for four different times (30, 60, 90, and 120 s from the start of the simulation). Every third cell is shown for the MODFLOW 6 results .....	5
8. Analytical and numerical solution (MODFLOW 6) for solute transport in a one-dimensional, steady flow field for a case with no dispersion. Results are shown for the three different advection schemes implemented in MODFLOW 6: central-in-space weighting, upstream weighting, and the TVD scheme. The number of cells used for this simulation is 31. Every third time step is shown for the MODFLOW 6 results .....	6
9. Analytical and numerical solution (MODFLOW 6) for solute transport in a one-dimensional, steady flow field for a case with no dispersion. Results are shown for the three different advection schemes implemented in MODFLOW 6: central-in-space weighting, upstream weighting, and the TVD scheme. The number of cells used for this simulation is 31. The concentration for every cell is shown for the MODFLOW 6 results .....	6
10. Model grid and boundary conditions used for the Henry problem. Freshwater inflow is specified for the cells shown in red on the left at a combined rate of $5.702 \text{ m}^3/\text{d}$ for the classic problem and $2.851 \text{ m}^3/\text{d}$ for a modified version of the problem. Cells shown in blue on the right side are specified as seawater hydrostatic conditions .....	7
11. Simulation results for the Henry Problem (top plot) and the modified Henry problem (bottom plot), in which the freshwater inflow rate is halved. For these simulations, the saltwater boundary is treated as a specified concentration boundary .....	8
12. Simulation results for the Henry Problem (top plot) and the modified Henry problem (bottom plot) in which the freshwater inflow rate is cut in half. For these simulations, the saltwater boundary is treated a mixed boundary condition in which inflowing water from an external saltwater reservoir enters the model domain at the concentration of saltwater, but if flow is out of the model, then the outflow is assigned the concentration of the model cell .....	10
13. Saltwater level as a function of time for the dynamic Henry problem with a fluctuating saltwater boundary .....	11
14. Model grid and boundary conditions used for the Henry problem with a dynamic saltwater boundary. Freshwater inflow is specified for the cells shown in red on the left at a combined rate of $1.426 \text{ m}^3/\text{d}$ . Cells shown in yellow on the right side are specified as drains with the drain elevation set to the cell elevation. Cells shown in cyan on the right side are specified as general-head boundaries with the head set from a sinusoidal saltwater level function .....	13
15. Simulated results for the Henry problem with a dynamic saltwater level. Plots are for (a) the end of the first period, where the saltwater level was held constant at $0.75 \text{ m}$ , (b) the first high saltwater level, which occurs at $0.312 \text{ d}$ , and (c) the first low saltwater level, which occurs at $0.437 \text{ d}$ . Contours represent relative salinity values and range from 0 (freshwater) to 1 (saltwater) .....	14
16. Diagram showing the configuration of the saltwater intrusion laboratory experiment conducted by Goswami and Clement (2007) .....	15
17. Comparison of model predicted 0.10, 0.50, and 0.90 relative salinity values for the steady state 2 experiment. Modified from Figure 6 of Goswami and Clement (2007) to include MODFLOW 6 results .....	16

18. Comparison of steady state model results against experimental data. Modified from Figure 5 of Goswami and Clement (2007) to include MODFLOW 6 results .....	17
19. Comparison of model predicted intruding salt wedge locations against experimental data. Modified from Figure 7 of Goswami and Clement (2007) to include MODFLOW 6 results .....	17
20. Comparison of model predicted receding salt wedge locations against experimental data. Modified from Figure 8 of Goswami and Clement (2007) to include MODFLOW 6 results .....	18

## Tables

Blank page

DRAFT: December 18, 2019

---PROVISIONAL---

This should not be referenced, cited, or  
released without USGS Bureau approval.

# Introduction

This document describes example problems for the Groundwater Transport (GWT) Model.

## Example Problems

### Problem 1—One-Dimensional Transport

This problem corresponds to the first problem presented in the MOC3D report [Konikow and others \(1996\)](#), which involves the transport of a dissolved constituent in a steady, one-dimensional flow field. An analytical solution for this problem is given by [Wexler \(1992\)](#).

The model grid for this problem consists of one layer, 120 rows, and 1 columns. The top for each cell is assigned a value of 1.0 cm and the bottom is assigned a value of zero. DELR is set to 1.0 cm and DELC is specified with a constant value of 0.1 cm. The simulation consists of one stress period that is 120 s in length, and the stress period is divided into 240 equally sized time steps. By using a uniform porosity value of 0.1, a velocity value of 0.1 cm/s results from the injection of water at a rate of 0.001 cm<sup>3</sup>/s into the first cell. The last cell is assigned a constant head with a value of zero, though this value is not important as the cells are marked as being confined. The concentration of the injected water is assigned a value of 1.0, and any water that leaves through the constant-head cell leaves with the simulated concentration of the water in that last cell. Advection is solved using the TVD scheme to reduce numerical dispersion.

Two different levels of dispersion were simulated, and these simulations are referred to as the low dispersion case and the high dispersion case. The low dispersion case has a dispersion coefficient of 0.01 cm<sup>2</sup>/s, which, for the specified velocity, corresponds to a dispersivity value of 0.1 cm. The high-dispersion case has a dispersion coefficient of 0.1 cm<sup>2</sup>/s, which corresponds to a dispersivity value of 1.0 cm.

A comparison between the analytical solution and the MODFLOW 6 simulation for the low dispersion case is shown in figure 1. This plot can be compared to figure 18 in [Konikow and others \(1996\)](#). The three separate concentration versus time curves represent the three different distances (0.05, 4.05, and 11.05 cm). For this low-dispersion case, the MODFLOW 6 solution does not show perfect agreement with the analytical solution. This is due primarily to limitations with the numerical solution method, which can suffer from numerical dispersion.

Results for the high dispersion case are shown in figure 2. This plot can be compared to figure 19 in [Konikow and others \(1996\)](#). As before, every fifth time step is shown for the MODFLOW 6 simulation. Agreement between the MODFLOW 6 results and the analytical solution is slightly better for this case with higher dispersion.

[Konikow and others \(1996\)](#) presented a detailed view of the concentration versus time for the first cell for times less than 10 seconds in their figures 20 and 21. Their purpose for showing the early time results was to evaluate the accuracy of the MOC method, which can exhibit spurious oscillations under some conditions. The detailed view of early time concentrations for the first cell is reproduced here in figure 3 for the MODFLOW 6 results to show that the TVD method implemented in MODFLOW 6 provides good agreement with the analytical solution, even for early times.

Comparisons between MODFLOW 6 and the analytical solution can also be shown as concentration versus distance for selected times. As shown by [Konikow and others \(1996\)](#) in their figure 22, the MODFLOW 6 results for the low dispersion case are presented here in figure 4. The discrepancy between the MODFLOW 6 results and the analytical solution is caused by numerical dispersion. As shown in figure 5, which is the concentration versus distance plot for the high-dispersion case, the agreement between MODFLOW 6 and the analytical solution is much better.

## 2 MODFLOW 6 Groundwater Transport Model Example Problems

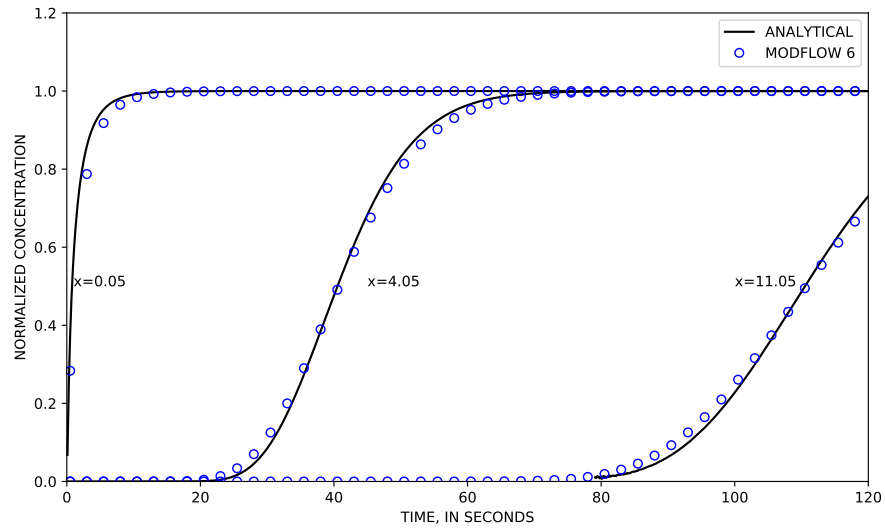


**Figure 1.** Analytical (Wexler, 1992) and numerical solution (MODFLOW 6) for solute transport in a one-dimensional, steady flow field for the low dispersion case ( $\alpha_L = 0.1 \text{ cm}$ ,  $D_{xx} = 0.01 \text{ cm}^2/\text{s}$ ). Results are shown for three different distances (0.05, 4.05, and 11.05 cm from the end of the first cell). Every fifth time step is shown for the MODFLOW 6 results.

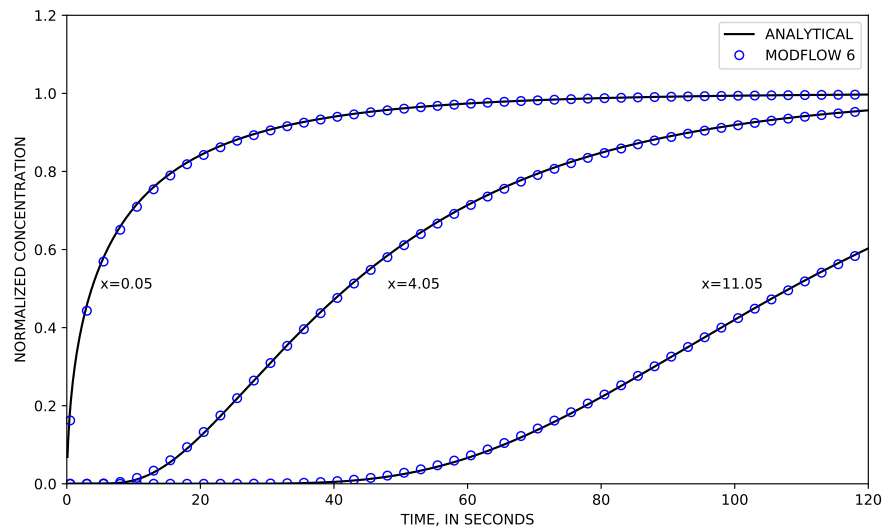


**Figure 2.** Analytical (Wexler, 1992) and numerical solution (MODFLOW 6) for solute transport in a one-dimensional, steady flow field for the high dispersion case ( $\alpha_L = 1.0 \text{ cm}$ ,  $D_{xx} = 0.1 \text{ cm}^2/\text{s}$ ). Results are shown for three different distances (0.05, 4.05, and 11.05 cm from the end of the first cell). Every fifth time step is shown for the MODFLOW 6 results.

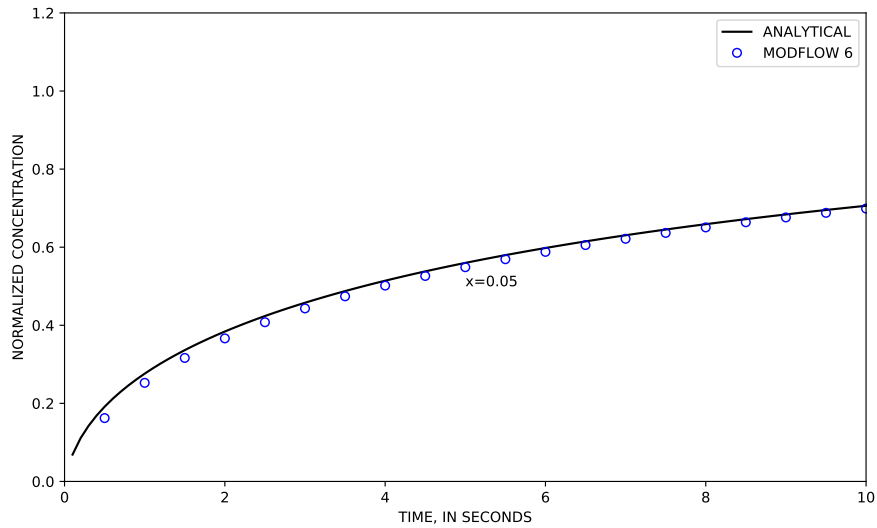


**Figure 3.** Detailed view of the analytical solution and MODFLOW 6 results for early times ( $t < 10$  s) at the first cell. Results are for the high dispersion case, as shown in figure 2. Every time step is shown for the MODFLOW 6 results.

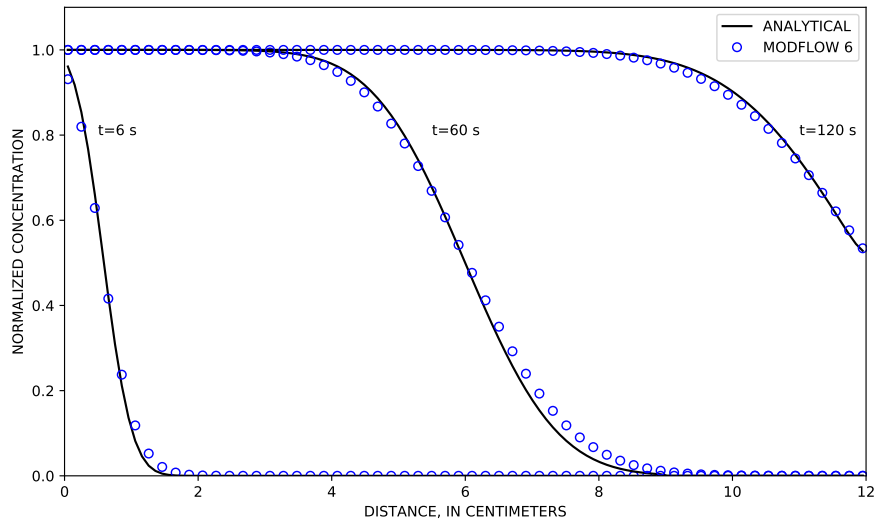


**Figure 4.** Analytical (Wexler, 1992) and numerical solution (MODFLOW 6) for solute transport in a one-dimensional, steady flow field for the low dispersion case ( $\alpha_L = 0.1$  cm,  $D_{xx} = 0.01$  cm $^2$ /s). Results are shown for three different times (6, 60, and 120 s from the start of the simulation). Every other cell is shown for the MODFLOW 6 results.

## 4 MODFLOW 6 Groundwater Transport Model Example Problems

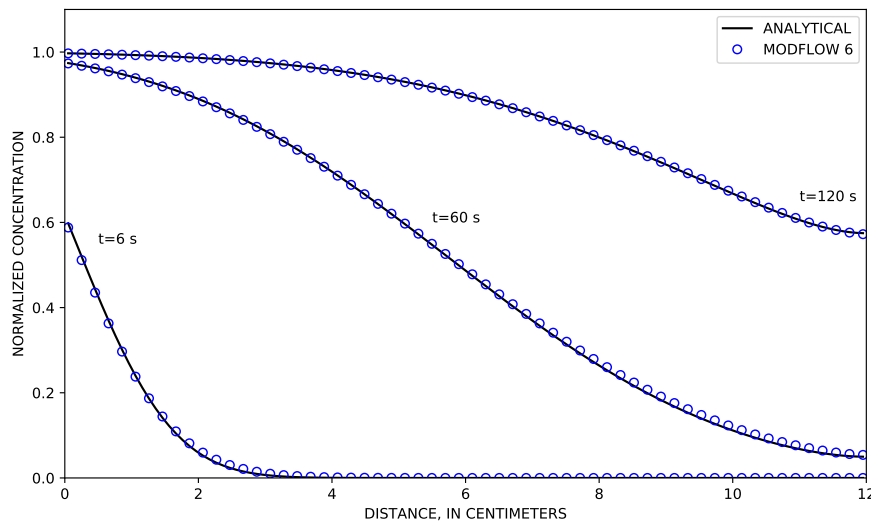


**Figure 5.** Analytical (Wexler, 1992) and numerical solution (MODFLOW 6) for solute transport in a one-dimensional, steady flow field for the high dispersion case ( $\alpha_L = 1.0 \text{ cm}$ ,  $D_{xx} = 0.1 \text{ cm}^2/\text{s}$ ). Results are shown for three different times (6, 60, and 120 s from the start of the simulation). Every other cell is shown for the MODFLOW 6 results.

The effect of first-order decay is simulated using a decay rate of  $\lambda = 0.01 \text{ s}^{-1}$ . Results for the low dispersion case are shown in figure 6, and the results for the high dispersion case are shown in figure 7. The numerical results are slightly better for the high dispersion case, compared to the low dispersion case, due to numerical dispersion in the solution.

A final example is shown here to demonstrate the effects of the different advection solution schemes in MODFLOW 6. This example is motivated by description of advection and corresponding breakthrough curves on pages 7–8 in Zheng and Wang (1999) and on pages 184–186 in Zheng and Bennett (2002). These schemes include central-in-space weighting, upstream weighting, and the TVD scheme. To accentuate the behavior of the schemes, the problem is modified by eliminating the intended dispersion so that all of the dispersion in the simulations is due to numerical dispersion. The analytical solution for these problems is calculated simply from a piston flow calculation in which the time to the concentration front is equal to the distance divided by the flow velocity. Figures 8 and 9 show concentration plots for this simulation with no intended dispersion. For this problem, the number of cells is set to an odd number (number of cells is 31) so that cell 16 is in the middle of the grid. The results for the three different schemes are very different. The central-in-space scheme exhibits numerical oscillations in which the simulated concentration can be larger than the specified inflow concentration; for this reason, the central-in-space weighting scheme is not normally used in practice. The upstream weighting scheme does not exhibit numerical oscillations, but it is subject to more numerical dispersion than the central-in-space and TVD schemes. The TVD scheme provides the best results for this problem.

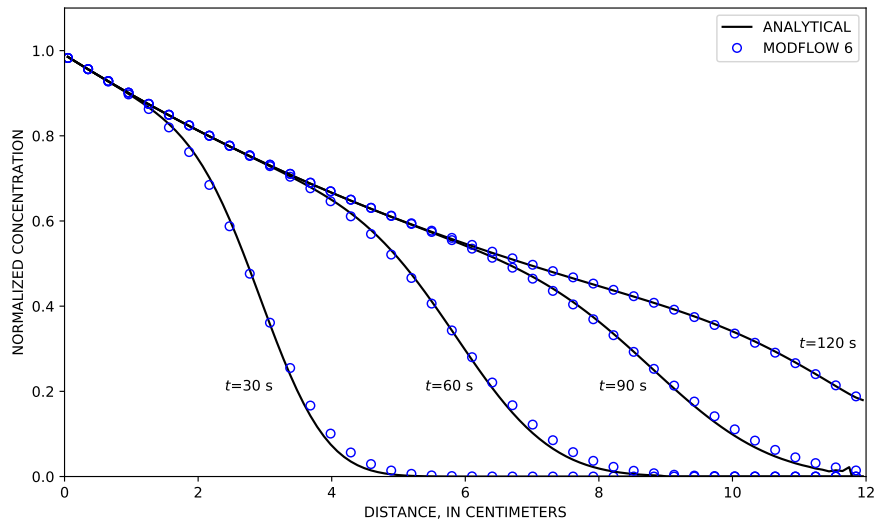


**Figure 6.** Analytical (Wexler, 1992) and numerical solution (MODFLOW 6) for solute transport in a one-dimensional, steady flow field for the low dispersion case ( $\alpha_L = 0.1 \text{ cm}$ ,  $D_{xx} = 0.01 \text{ cm}^2/\text{s}$ ) and with a first-order decay rate of  $\lambda = 0.01 \text{ s}^{-1}$ . Results are shown for four different times (30, 60, 90, and 120 s from the start of the simulation). Every third cell is shown for the MODFLOW 6 results.

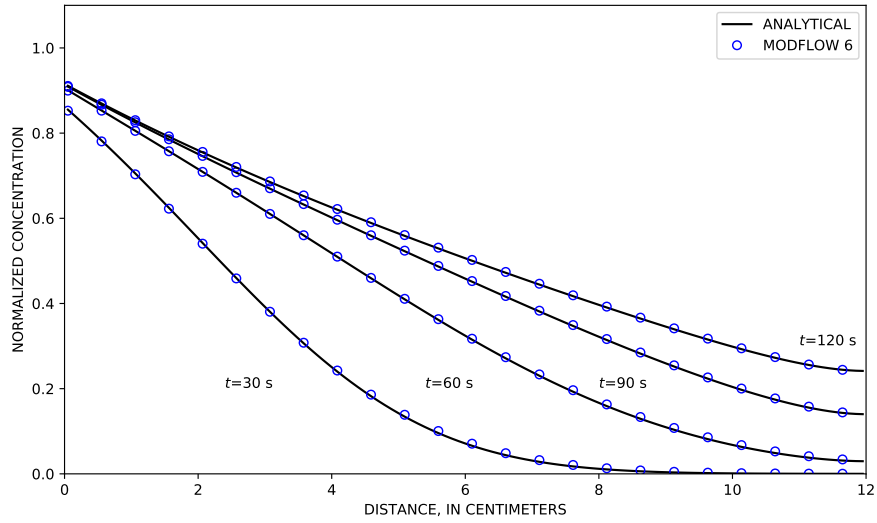


**Figure 7.** Analytical (Wexler, 1992) and numerical solution (MODFLOW 6) for solute transport in a one-dimensional, steady flow field for the high dispersion case ( $\alpha_L = 1.0 \text{ cm}$ ,  $D_{xx} = 0.1 \text{ cm}^2/\text{s}$ ) and with a first-order decay rate of  $\lambda = 0.01 \text{ s}^{-1}$ . Results are shown for four different times (30, 60, 90, and 120 s from the start of the simulation). Every third cell is shown for the MODFLOW 6 results.

## 6 MODFLOW 6 Groundwater Transport Model Example Problems

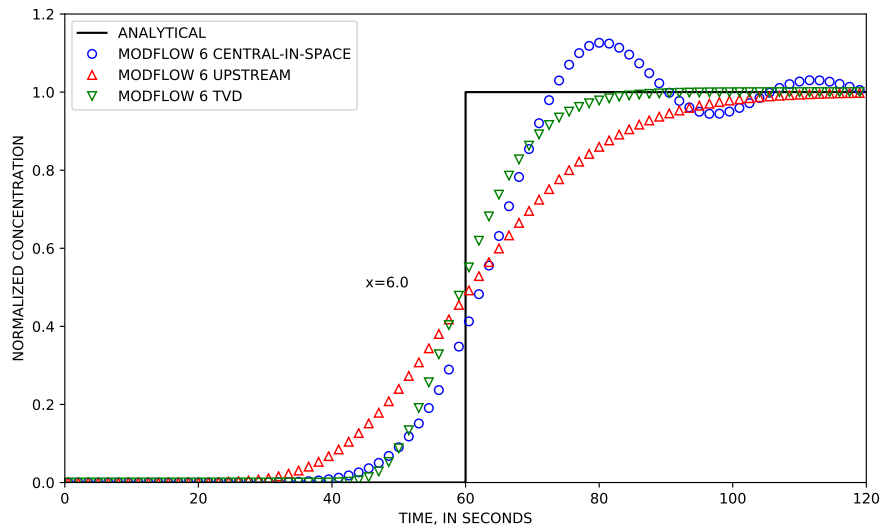


**Figure 8.** Analytical and numerical solution (MODFLOW 6) for solute transport in a one-dimensional, steady flow field for a case with no dispersion. Results are shown for the three different advection schemes implemented in MODFLOW 6: central-in-space weighting, upstream weighting, and the TVD scheme. The number of cells used for this simulation is 31. Every third time step is shown for the MODFLOW 6 results.

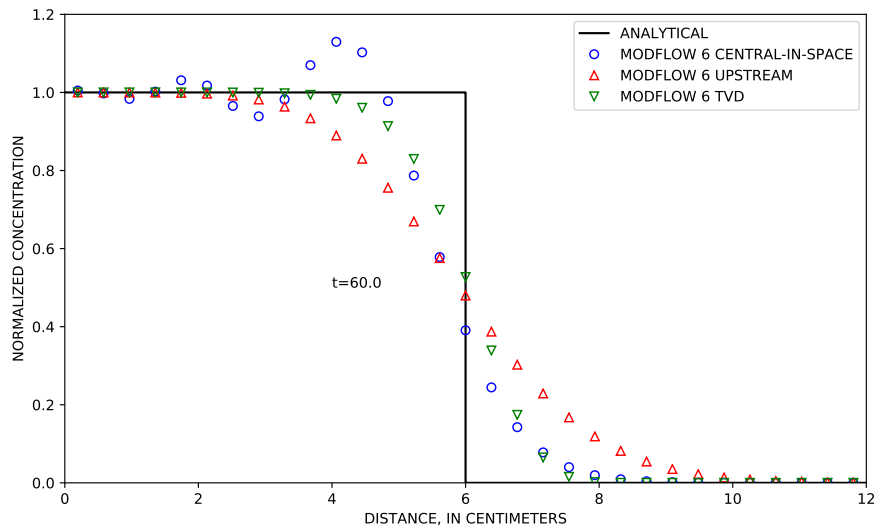


**Figure 9.** Analytical and numerical solution (MODFLOW 6) for solute transport in a one-dimensional, steady flow field for a case with no dispersion. Results are shown for the three different advection schemes implemented in MODFLOW 6: central-in-space weighting, upstream weighting, and the TVD scheme. The number of cells used for this simulation is 31. The concentration for every cell is shown for the MODFLOW 6 results.

## Problem 11–Henry Problem

The Henry problem (Henry, 1964) is commonly used as a benchmark test problem to ensure that variable-density flow and transport codes are working properly. The problem consists of a 2-m long by 1-m tall simulation domain (fig. 10). Freshwater with a density value of  $1000 \text{ kg/m}^3$  flows into the domain through the left side at a rate of  $5.7024 \text{ m}^3/\text{d}$  for the classic version of the problem and at a rate of  $2.851 \text{ m}^3/\text{d}$  for a modified version of the problem described by Simpson and Clement (2004). The modified version of the problem provides a better benchmark test of the density terms than the classic problem. A hydrostatic saltwater boundary is assigned to the right side with a prescribed salt concentration of  $35 \text{ kg/m}^3$  and density of  $1024.5 \text{ kg/m}^3$ . The transport boundary for the saltwater side can be represented in a couple of different ways. It can be set as a fixed concentration, whereby advection and diffusion occur at the boundary. It can also be set as a mixed boundary condition, whereby inflowing water from the boundary enters the model domain at the concentration of saltwater, but if flow is out of the model domain, then the outflow is assigned the concentration of the model domain at that location. Both types of boundary are evaluated here. A freshwater hydraulic conductivity value of  $864 \text{ m/d}$  is used; porosity is assigned a value of 0.35. Mechanical dispersion is not represented. Instead all mixing occurs through simple diffusion that is represented using a molecular diffusion coefficient of  $1.62925 \text{ m}^2/\text{d}$ . For the testing described here, the domain is divided into 40 layers and 80 columns. The simulation begins with the domain initially filled with saltwater. A simulation period of  $0.5 \text{ d}$  is divided into 500 equally sized time steps of  $0.001 \text{ d}$ .

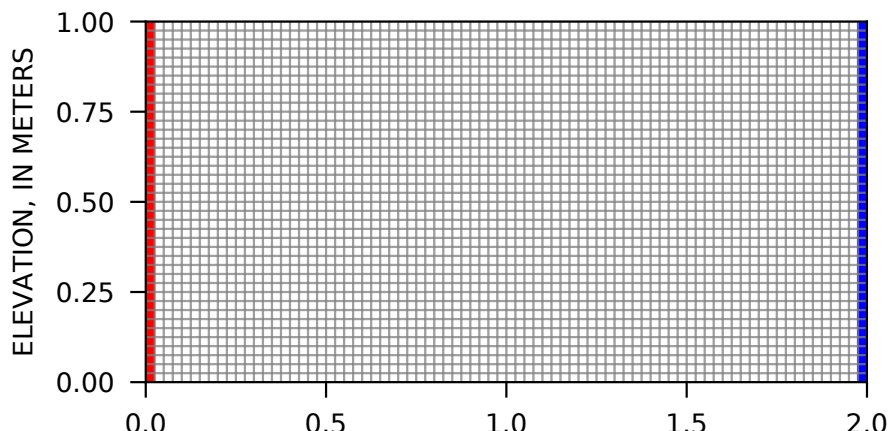


**Figure 10.** Model grid and boundary conditions used for the Henry problem. Freshwater inflow is specified for the cells shown in red on the left at a combined rate of  $5.702 \text{ m}^3/\text{d}$  for the classic problem and  $2.851 \text{ m}^3/\text{d}$  for a modified version of the problem. Cells shown in blue on the right side are specified as seawater hydrostatic conditions.

Results from the classic and modified Henry problem in which the saltwater boundary is represented in the last column of model cells as a constant head and constant concentration are shown in Figure 11 for the end of the  $0.5 \text{ d}$  simulation period. Contours of relative salinity fraction are shown for values of 0.01, 0.1, 0.5, 0.9, and 0.99. There is very good agreement between the MODFLOW 6 hydraulic head formulation, and the SEAWAT equivalent freshwater head formulation.

Results from the classic and modified Henry problem in which the saltwater boundary is represented as mixed boundary condition are shown in Figure 12 for the end of the  $0.5 \text{ d}$  simulation period. For these simulations, the saltwater boundary is represented with the General-Head Boundary (GHB) Package. Conceptually, a saltwater reservoir is attached to the edge of each model cell in the last column. If there is flow into the model domain, then that flow enters at a density of saltwater. Alternatively, if flow is out of the model domain, then flow exiting the system leaves with the density of the cell in the last column. This manner of representing the

## 8 MODFLOW 6 Groundwater Transport Model Example Problems

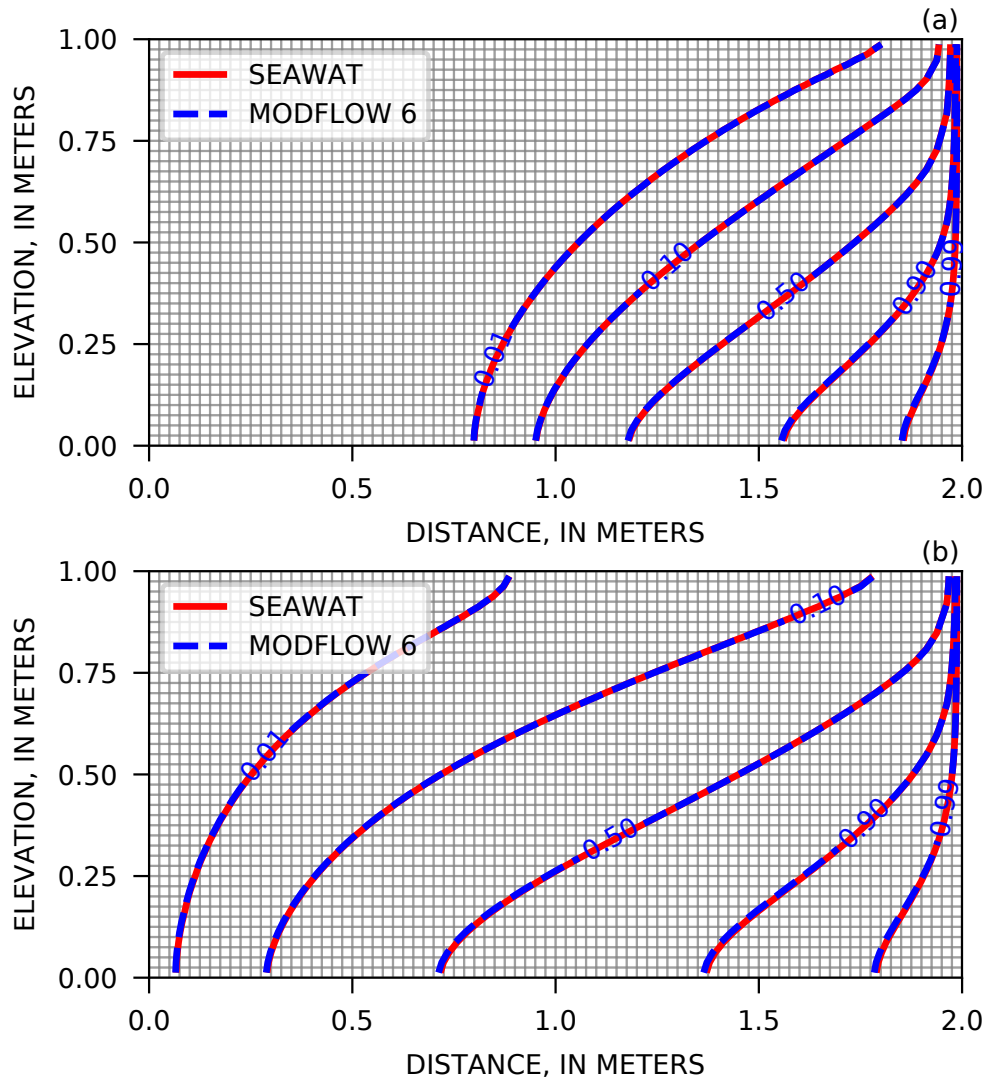


**Figure 11.** Simulation results for the Henry Problem (top plot) and the modified Henry problem (bottom plot), in which the freshwater inflow rate is halved. For these simulations, the saltwater boundary is treated as a specified concentration boundary.

saltwater boundary is often used for saltwater intrusion models, and allows a freshwater outflow zone to form. Contours of relative salinity fraction are shown for values of 0.01, 0.1, 0.5, 0.9, and 0.99. As with the constant head and constant concentration simulations, there is very good agreement between the MODFLOW 6 hydraulic head formulation, and the SEAWAT equivalent freshwater head formulation.

## 10 MODFLOW 6 Groundwater Transport Model Example Problems

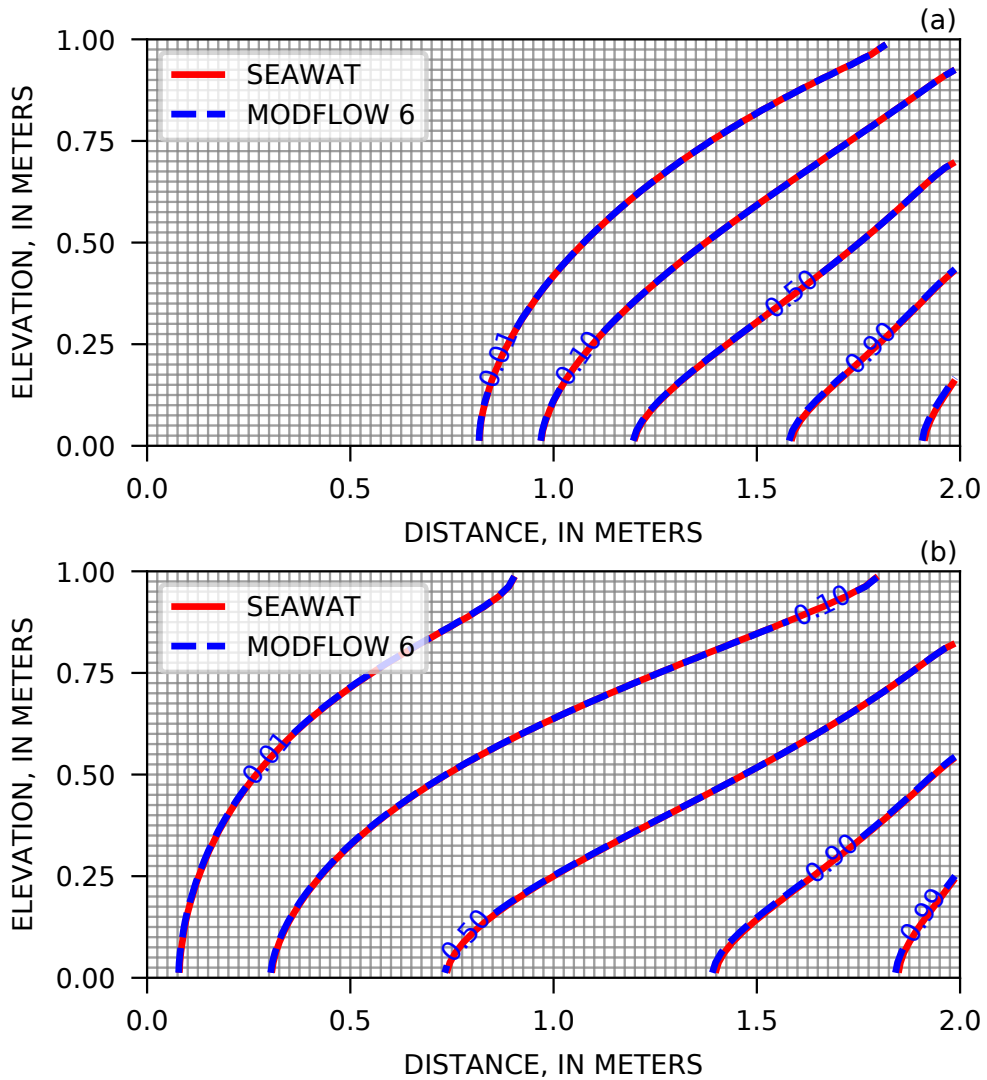


**Figure 12.** Simulation results for the Henry Problem (top plot) and the modified Henry problem (bottom plot) in which the freshwater inflow rate is cut in half. For these simulations, the saltwater boundary is treated a mixed boundary condition in which inflowing water from an external saltwater reservoir enters the model domain at the concentration of saltwater, but if flow is out of the model, then the outflow is assigned the concentration of the model cell.

## Problem 12–Fluctuating Saltwater Boundary

The density dependent hydraulic head formulation can be used with the Newton-Raphson Formulation to simulate the rise and fall of the water table over multiple layers of model cells. The Henry problem described in the previous example is modified to include a fluctuating saltwater boundary imposed on a sloped surface. This simulation is designed to represent the groundwater flow processes that might be observed in a coastal aquifer affected by tidal fluctuations or longer term changes in sea level. Approaches for representing these types of fluctuations with a variable-density groundwater model is described by [Mulligan and others \(2011\)](#).

The simulation is designed to represent a 1.25-*d* time period. The first stress period is 0.25 *d*, has a constant sea level elevation of 0.85 *m*, and has time steps equal to 0.001 *d*. During this first stress period, the saltwater level is held constant at 0.85 *m*. The remainder of the simulation consists of 1000 stress periods, each having a single time step with a length of 0.001 *d*. During this 1-*d* period, the saltwater level is represented using a sinusoidally varying function that has an amplitude of 0.14 *m*, a frequency of 4 /*d*, and a shift of 0.85 *m* as shown in Figure 13. For the entire simulation period, a freshwater inflow rate of 1.425 *m*<sup>3</sup>/*d* is specified for the left boundary. This freshwater inflow rate, which is one fourth the rate used for the classic Henry problem, was used in order to keep all of the saltwater from being flushed out of the domain.

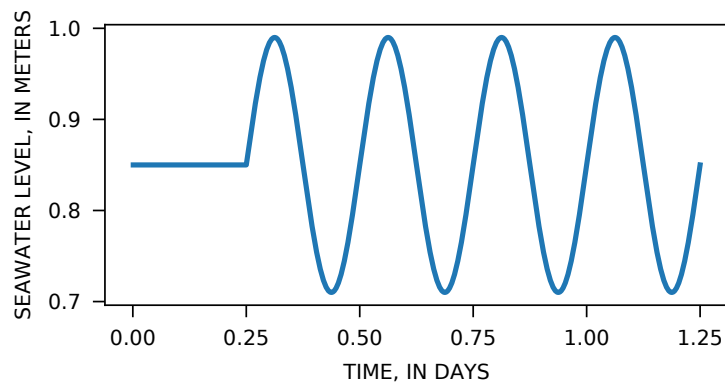


**Figure 13.** Saltwater level as a function of time for the dynamic Henry problem with a fluctuating saltwater boundary.

The parameters for the simulation, including the size and shape of the model domain, are patterned after the Henry problem, except that the saltwater boundary is applied to a sloped surface as shown in Figure 14. Cells above the sloped surface are not included in the simulation. Cells defining the sloped surface that are inundated by saltwater are assigned a general-head boundary with the head set to the saltwater level. Cells along the sloped surface that are above the saltwater level are assigned a drain condition with the elevation of the drain equal to the cell elevation. This is an approach described by [Mulligan and others \(2011\)](#) to simulate tidal boundary conditions with SEAWAT. For the second part of the simulation in which the saltwater level is varying according to Figure 13, the drains and general-head boundaries are reassigned each stress period as the saltwater level rises and falls. For example, as shown in Figure 14, at the mean saltwater level of 0.85 *m*, there are 7 layers of cells along the sloped surface that have drains assigned to them. The elevations of these cells are above the saltwater level. The remaining cells along the sloped boundary with elevations lower than the mean saltwater level are assigned general head boundaries. Figure 13 also shows the boundary configurations for the maximum and minimum saltwater levels.

Selected results from the Henry problem with a dynamic saltwater level are shown in Figure 15 for three different times representing (1) the end of the first stress period in which the saltwater level was held constant at the mean value, (2) the first high saltwater level at 0.312 *d*, and (3) the first low saltwater level at 0.437 *d*. Cells shown in gray are considered dry in that their calculated hydraulic head value is below the cell bottom elevation; in this simulation, the head values of dry cells are equal to the water table elevation. This type of

## **12 MODFLOW 6 Groundwater Transport Model Example Problems**

fluctuating boundary in which the water table rises and falls over multiple model layers is difficult to simulate with a saturated groundwater model unless a Newton-Raphson formulation is used. For example, it is difficult and often not possible to use the SEAWAT program for this type of problem, because SEAWAT is based on the traditional wetting and drying formulation in MODFLOW which is highly unstable and often does not converge.

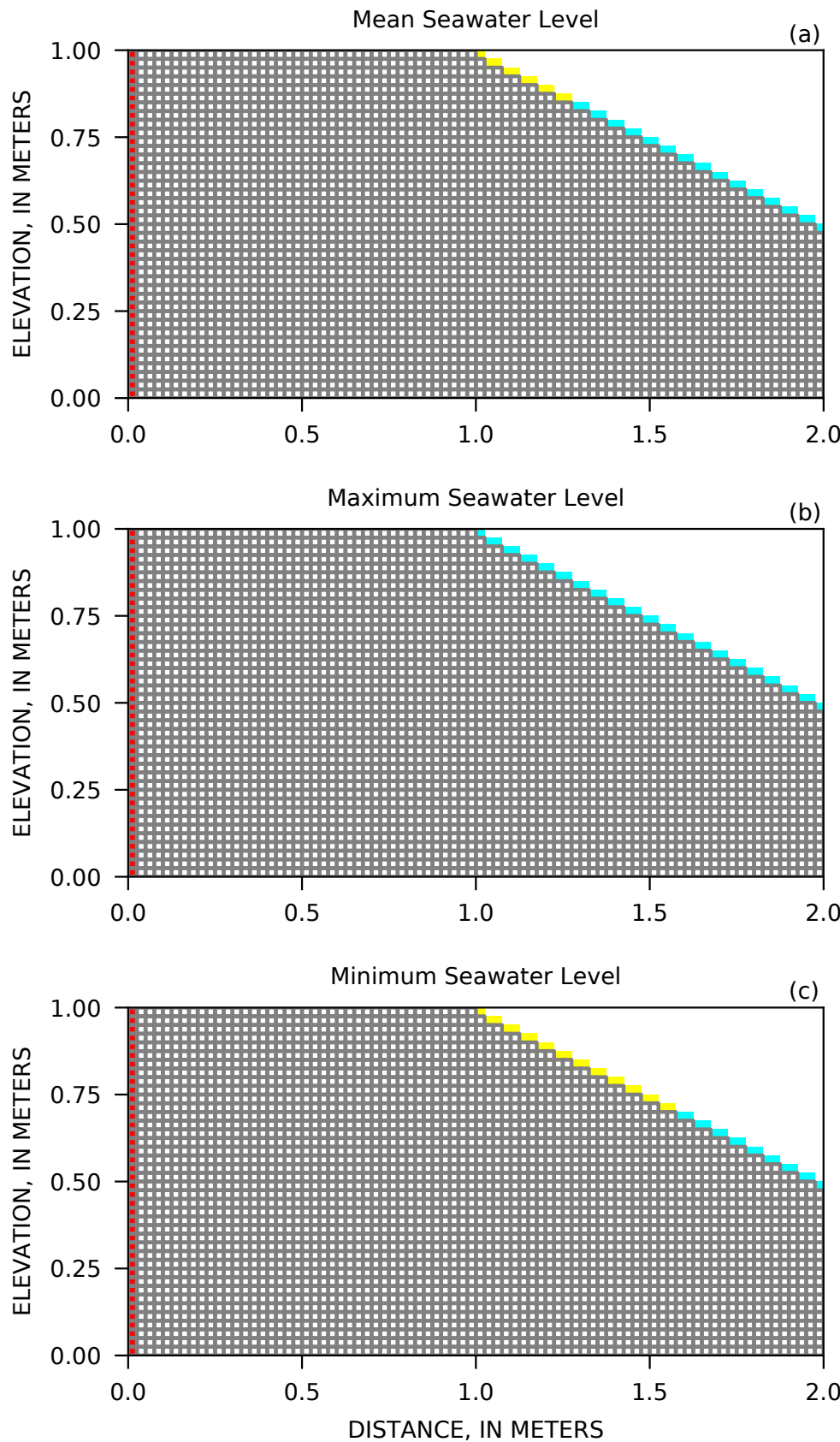


**Figure 14.** Model grid and boundary conditions used for the Henry problem with a dynamic saltwater boundary. Freshwater inflow is specified for the cells shown in red on the left at a combined rate of  $1.426 \text{ m}^3/\text{d}$ . Cells shown in yellow on the right side are specified as drains with the drain elevation set to the cell elevation. Cells shown in cyan on the right side are specified as general-head boundaries with the head set from a sinusoidal saltwater level function.

DRAFT: December 18, 2019 This should not be referenced, cited, or released without USGS Bureau approval.

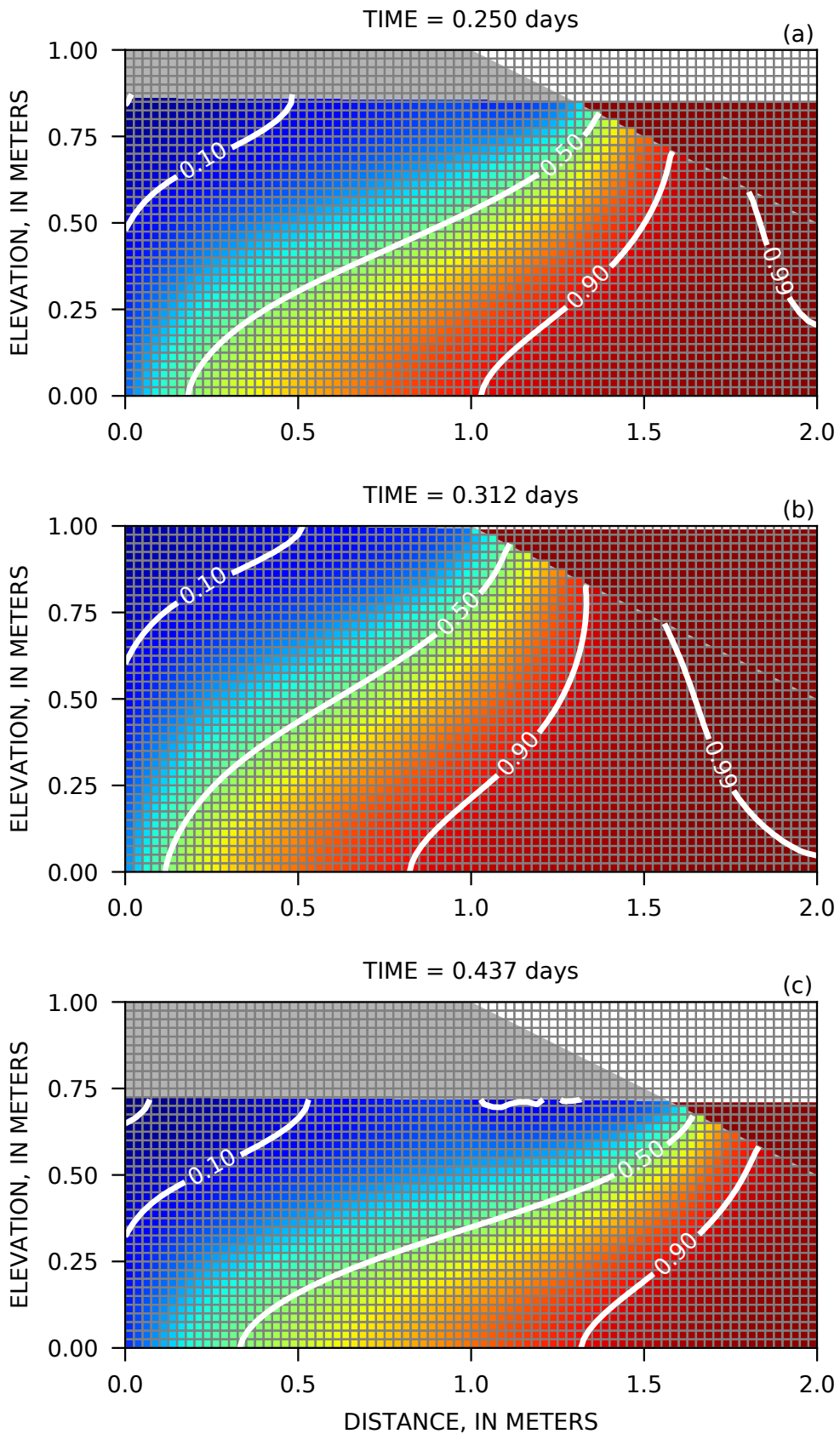


**Figure 15.** Simulated results for the Henry problem with a dynamic saltwater level. Plots are for (a) the end of the first period, where the saltwater level was held constant at 0.75 m, (b) the first high saltwater level, which occurs at 0.312 d, and (c) the first low saltwater level, which occurs at 0.437 d. Contours represent relative salinity values and range from 0 (freshwater) to 1 (saltwater).

## Problem 13–Saltwater Intrusion Dynamics

Simpson and Clement (2004) suggest that benchmarking problems be used to test numerical codes that are sensitive to coupling between flow and transport. Goswami and Clement (2007) proposed such an experimental study for benchmarking variable-density codes. They conducted experiments in a rectangular flow tank with internal dimensions of 53 cm (length) by 30.5 cm (height) by 2.7 cm (width). The formation and movement of saltwater wedges were represented in the experiment by applying a constant head saltwater boundary (density = 1.026 g/ml) on the left side of the tank and a constant head freshwater boundary (density = 1.000 g/ml) on the right side of the tank. A schematic of the laboratory experiment in shown in Figure 16. To start the experiment, the system was allowed to equilibrate with a freshwater head of 26.7 cm applied to the right boundary. Upon reaching steady state, this condition is called the SS-1. Next, the freshwater head was lowered to 26.2 cm and saltwater was allowed to advance into the tank, and movement of the interface between freshwater and saltwater was recorded. After about 80 min, the system reached steady state. This condition is referred to as SS-2. Lastly, the freshwater head was raised to 26.55 cm, which caused the interface between freshwater and saltwater to recede, and once again, the movement was recorded. This final condition is referred to as SS-3. Data for these three steady state positions, the advancing and retreating interface positions, and the freshwater inflow rates for the three steady state conditions are reported in Goswami and Clement (2007). Goswami and Clement (2007) also simulated the experiment using the SEAWAT code, and showed that it is capable of simulating saltwater intrusion dynamics.

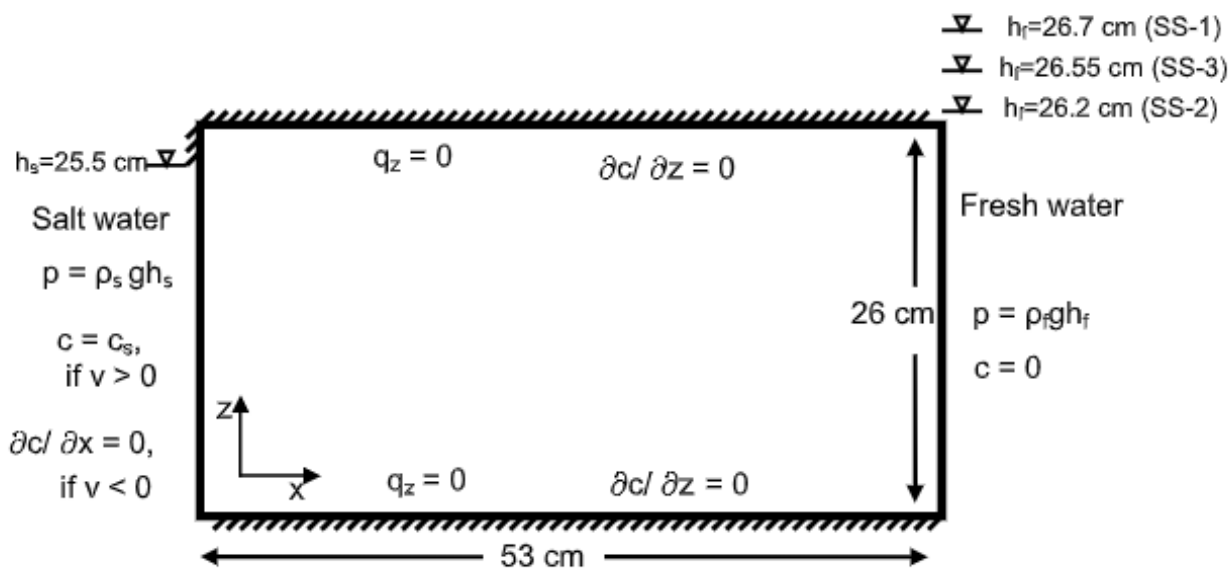


**Figure 16.** Diagram showing the configuration of the saltwater intrusion laboratory experiment conducted by Goswami and Clement (2007).

A MODFLOW 6 model was developed to simulate the saltwater intrusion experiment of Goswami and Clement (2007). The model was constructed using a 0.5 cm grid. The saltwater boundary on the left side of the tank was represented using general head boundaries. The freshwater boundary on the right side of the tank was represented as constant heads, with a different head value assigned to each stress period. The remaining parameter values, such as assignment of a hydraulic conductivity value equal to 1050 m/d and porosity value of 0.385, were set to be consistent with those presented in Goswami and Clement (2007) for the experiment and for the SEAWAT representation. Three stress periods are used to represent (1) equilibration to the SS-1 position, (2) advancing movement of the interface to SS-2, and (3) receding movement of the interface to SS-3.

## 16 MODFLOW 6 Groundwater Transport Model Example Problems

3. These stress periods are represented with 60, 80, and 60 *min*, respectively, with 1-second time steps.

Compared to SEAWAT, the results from MODFLOW 6 have a higher level of numerical dispersion. This is because the explicit third-order TVD scheme in MT3D, upon which SEAWAT is based, is better at maintaining sharp concentration fronts, such as those observed in the laboratory experiment, than the implicit second-order TVD scheme implemented in MODFLOW 6. In both the SEAWAT and MODFLOW 6 simulations, molecular diffusion and hydrodynamic dispersion is not represented, which means that any mixing observed in the simulations is due to numerical dispersion. Figure 17 shows the width of the simulated transition zone between freshwater and saltwater for the SS-2 condition. The width shown here for the MODFLOW 6 simulation is as large as about 5 cm, whereas the width for the SEAWAT simulation is about 1 cm. For benchmarking of the SEAWAT code, [Goswami and Clement \(2007\)](#) used a 0.5 relative salinity contour to compare with the measured interface positions; however, in the examples shown here, the simulated 0.2 relative salinity contour seems to be more representative of the laboratory experiment, and is used in the subsequent figures.

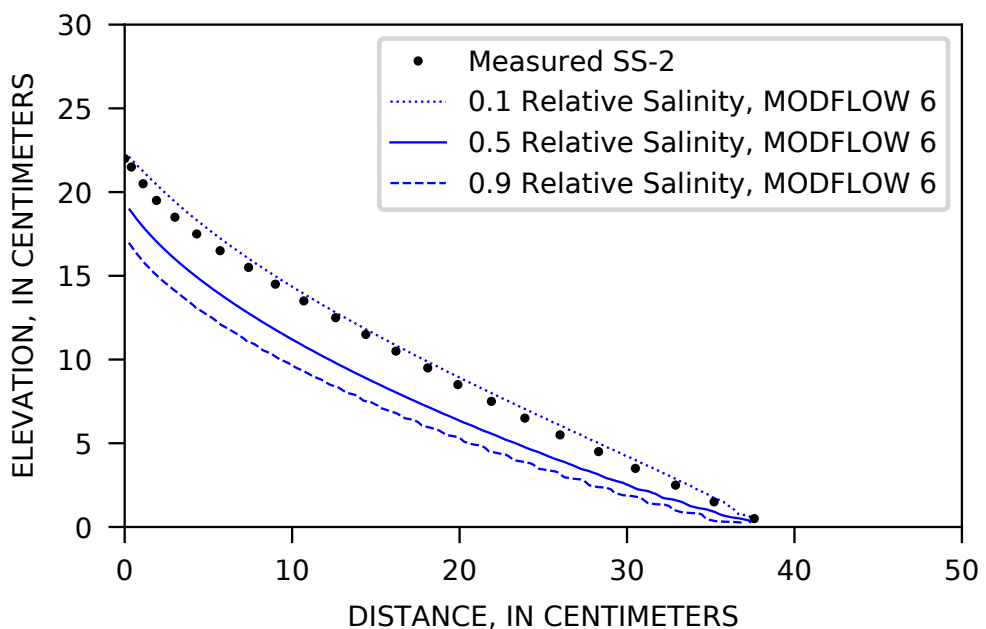


**Figure 17.** Comparison of model predicted 0.10, 0.50, and 0.90 relative salinity values for the steady state 2 experiment. Modified from Figure 6 of [Goswami and Clement \(2007\)](#) to include MODFLOW 6 results.

Figure 18 presents the comparison of numerical results with experimental data for the three steady state conditions. Results from the transient advancing and transient receding saltwater interfaces are presented in Figures 19 and 20, respectively. In addition to the interface positions, the simulated freshwater inflow rates for the three steady state conditions are also in good agreement with the freshwater inflow rates measured as part of the experiment. For SS-1, the measured and simulated freshwater inflow rates are 1.42 and 1.41  $cm^3/s$ , respectively. For SS-2, the measured and simulated freshwater inflow rates are 0.59 and 0.60  $cm^3/s$ , respectively. For SS-3, the measured and simulated freshwater inflow rates are 1.19 and 1.17  $cm^3/s$ , respectively. Simulation results from the MODFLOW 6 simulations generally compare well with experimental data showing the suitability of the code to represent saltwater intrusion dynamics.

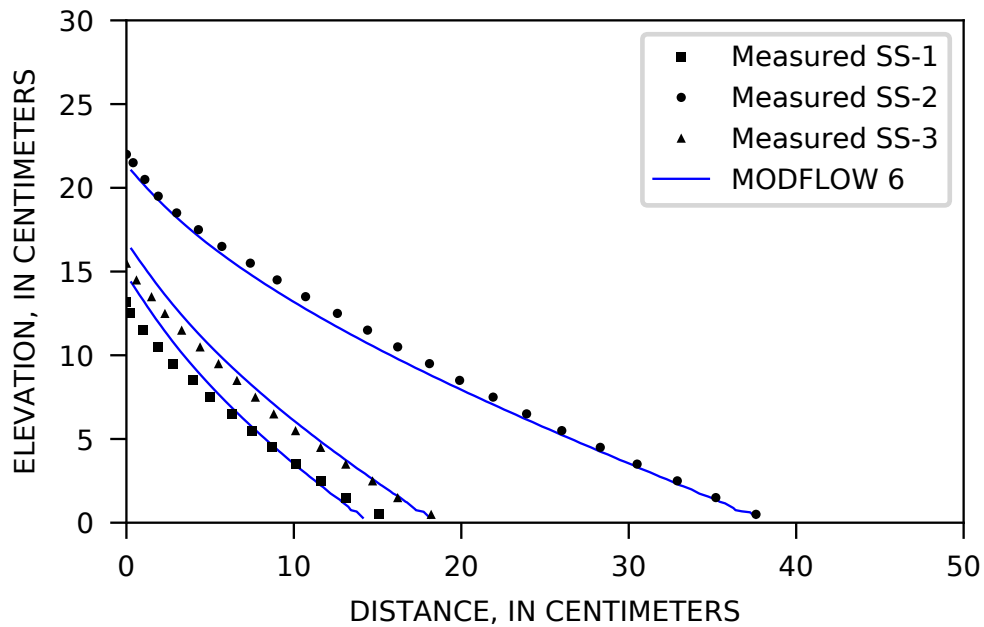


**Figure 18.** Comparison of steady state model results against experimental data. Modified from Figure 5 of [Goswami and Clement \(2007\)](#) to include MODFLOW 6 results.

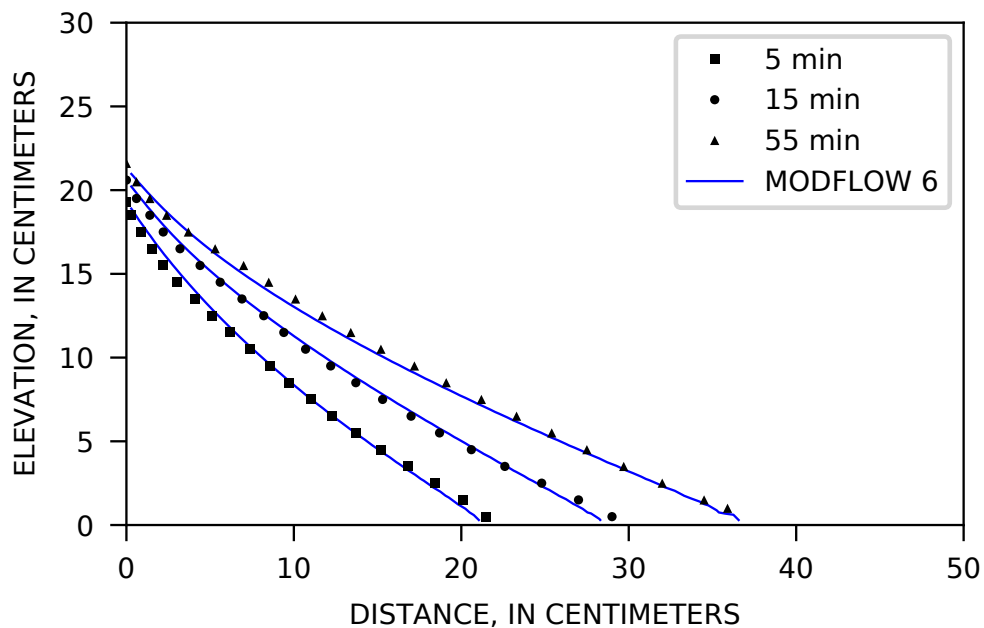


**Figure 19.** Comparison of model predicted intruding salt wedge locations against experimental data. Modified from Figure 7 of [Goswami and Clement \(2007\)](#) to include MODFLOW 6 results.

## 18 MODFLOW 6 Groundwater Transport Model Example Problems

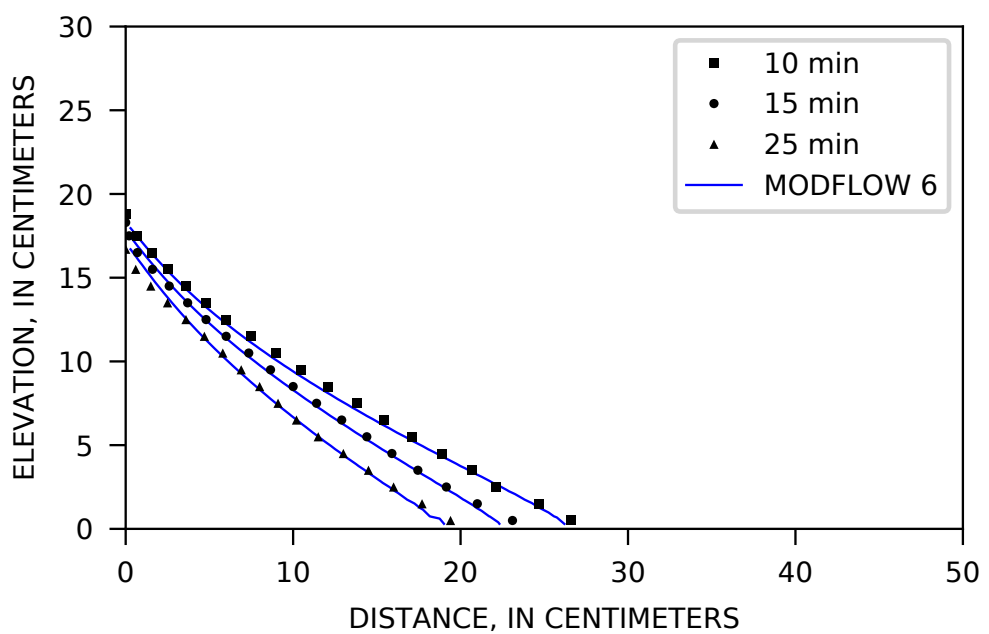


**Figure 20.** Comparison of model predicted receding salt wedge locations against experimental data. Modified from Figure 8 of Goswami and Clement (2007) to include MODFLOW 6 results.

## References Cited

- Goswami, R.R., and Clement, Prabhakar, 2007, Laboratory-scale investigation of saltwater intrusion dynamics: Water Resources Research, v. 43, no. W04418, <https://doi.org/10.1029/2006WR005151>.
- Henry, H.R., 1964, Effects of dispersion on salt encroachment in coastal aquifers: Sea Water in Coastal Aquifers, U.S. Geol. Surv. Supply Pap., 1613-C, C71-C84.
- Konikow, L.F., Goode, D.J., and Hornberger, G.Z., 1996, A three-dimensional method-of-characteristics solute-transport model (MOC3D): U.S. Geological Survey Water-Resources Investigations Report 96-4267, 87 p., accessed June 27, 2017, at <https://pubs.er.usgs.gov/publication/wri964267>.
- Mulligan, A.E., Langevin, C.D., and Post, V. E.A., 2011, Tidal boundary conditions in SEAWAT: Groundwater, v. 46, no. 6, p. 866–879, accessed July 11, 2019, at <https://ngwa.onlinelibrary.wiley.com/doi/pdf/10.1111/j.1745-6584.2010.00788.x>.
- Simpson, M.J., and Clement, T.P., 2004, Improving the worthiness of the Henry problem as a benchmark for density-dependent groundwater flow models: Water Resources Research, v. 40, no. W01504, p. 1152–1173, accessed July 1, 2019, at <https://doi.org/10.1029/2003WR002199>.
- Wexler, E.J., 1992, Analytical solutions for one-, two-, and three-dimensional solute transport in ground-water systems with uniform flow: U.S. Geological Survey Techniques of Water-Resources Investigations, Book 3, Chapter B7, 190 p.
- Zheng, Chunmiao, and Bennett, G.D., 2002, Applied contaminant transport modeling, 2nd edition: New York, New York, Wiley-Interscience, 560 p.
- Zheng, Chunmiao, and Wang, P.P., 1999, MT3DMS—A modular three-dimensional multi-species transport model for simulation of advection, dispersion and chemical reactions of contaminants in groundwater systems; Documentation and user's guide: Contract report SERDP-99-1: Vicksburg, Miss., U.S. Army Engineer Research and Development Center, 169 p.

DRAFT: December 18, 2019

---PROVISIONAL---

This should not be referenced, cited, or  
released without USGS Bureau approval.

Publishing support provided by the U.S. Geological Survey  
MODFLOW 6 Development Team

For information concerning this publication, please contact:

Office of Groundwater  
U.S. Geological Survey  
Mail Stop 411  
12201 Sunrise Valley Drive  
Reston, VA 20192  
(703) 648-5001  
<https://water.usgs.gov/ogw/>

DRAFT: December 18, 2019

---PROVISIONAL---

This should not be referenced, cited, or  
released without USGS Bureau approval.

<https://doi.org/10.5066/F76Q1VQV>

DRAFT: December 18, 2019

---PROVISIONAL---

This should not be referenced, cited, or  
released without USGS Bureau approval.